Submitted to Physics of Fluids

UCRL-19412
Preprint

c.2

MICROSCOPIC THEORY OF A MULTICOMPONENT SYSTEM OF CHARGED AND NEUTRAL PARTICLES. II. INVESTIGATION OF PROPERTIES OF PHOTONS

RECEIVED
LAWRENCE
RADIATION LABORATORY
MAY 13 1970
LIBRARY AND
DOCUMENTS SECTION

Anup Bhowmik and Charles Ray Smith

March 3, 1970

AEC Contract No. W-7405-eng-48

TWO-WEEK LOAN COPY

This is a Library Circulating Copy which may be borrowed for two weeks. For a personal retention copy, call Tech. Info. Division, Ext. 5545

UCRL-19412

LAWRENCE RADIATION LABORATORY
UNIVERSITY of CALIFORNIA BERKELEY

DISCLAIMER

This document was prepared as an account of work sponsored by the United States Government. While this document is believed to contain correct information, neither the United States Government nor any agency thereof, nor the Regents of the University of California, nor any of their employees, makes any warranty, express or implied, or assumes any legal responsibility for the accuracy, completeness, or usefulness of any information, apparatus, product, or process disclosed, or represents that its use would not infringe privately owned rights. Reference herein to any specific commercial product, process, or service by its trade name, trademark, manufacturer, or otherwise, does not necessarily constitute or imply its endorsement, recommendation, or favoring by the United States Government or any agency thereof, or the Regents of the University of California. The views and opinions of authors expressed herein do not necessarily state or reflect those of the United States Government or any agency thereof or the Regents of the University of California.

MICROSCOPIC THEORY OF A MULTICOMPONENT SYSTEM OF CHARGED AND NEUTRAL PARTICLES. II. INVESTIGATION OF PROPERTIES OF PHOTONS*†

Anup Bhowmik and Charles Ray Smith

Physics Department
University of Wyoming
Laramie, Wyoming 82070

March 3, 1970

ABSTRACT

On the basis of the Mohling-Smith generalized master-graph formulation of quantum statistics, the properties of photons in a non-relativistic, multicomponent fully ionized gas in thermal equilibrium are investigated. The photon self-energy is calculated by summation, to all orders, of selected diagrams, and it is proposed that the solution is formally exact. Next, the photon momentum distribution is calculated, in the high-temperature, low-density limit, to second order in the fine-structure constant. Several nonperturbative results are obtained which are significant even in lowest order. The lowest-order results have an interesting relation to the pair-Hamiltonian approximation and the Bogoliubov transformation, and this relation is discussed. Finally, the counterterm technique of the generalized master-graph theory is employed to accomplish mass-renormalization through second order in the fine-structure constant. The investigation is valid for particle densities $\rho \ll 10^{24}$ particles/cm^3 and for absolute temperatures $T \leq 10^6$ °K (but large enough for a high degree of ionization).

I. INTRODUCTION

It is reasonable to expect that quantum mechanics and quantized Maxwell-Lorentz electrodynamics can serve as a basis for a microscopic theory for calculating accurately the properties of a non-relativistic fully ionized gas in thermal equilibrium. In a previous paper[1] such a theory was proposed, where the goal has been to develop a theory that is not only rigorous, but also is tractable in practice.

Three type of divergences are prominent in a many-body theory of the equilibrium fully ionized gas: the ultraviolet, the Coulomb, and the infrared divergences--all are of electromagnetic origin. Thus, we are concerned with developing techniques for dealing with these divergences. The counterterm technique developed in I can be used to remove the ultraviolet divergence by means of mass-renormalization, and the Coulomb divergence has been effectively approached by selective summation of the so-called ring diagrams.[2] In a nonrelativistic theory, the infrared divergence has not yet been eliminated in a fundamental manner. In this paper, we avoid certain perturbation theoretic difficulties arising from the infrared divergence by finding non-iterative solutions or by selective summations of diagrams. In some applications the infrared divergence can be isolated by a Bogoliubov transformation of the photon operators, and relevant aspects of this technique will be discussed.

For the system of interest in this paper, there has been considerable activity directed toward the calculation of the photon momentum distribution in the high-temperature, low-density region;[3-8]

of course, a comprehensive treatment has not yet been achieved owing to the inherent complexity of the problem. Several of the recent investigations[4-7] have been based on the master-graph formalism of MG, and a renewed interest in the problem was created by the discovery that MG is substantially in error for certain self-energy structures [called (2,0) and (0,2) structures]. These self-energy structures are included properly in I, and it is of interest in this paper to use the generalized master-graph theory of I to learn the effects of a complete photon self-energy analysis on previous results. Also, it is of interest to explore the usefulness of the counterterm technique given in I.

In this paper we present results of calculations of the photon self-energy and momentum distribution. Thus, in Sec. II we give necessary preliminary details about the system. In Sec. III we outline the calculation of the photon self-energy; the result obtained is based on an extensive partial summation procedure, and it is suggested that our solution may be formally exact. Next, in Sec. IV, we calculate the photon momentum distribution to second order in the fine-structure constant. In both Secs. III and IV, the effects of the (2,0) and (0,2) structures are investigated. In the final section, Sec. V, we summarize the general nature of these studies. The counterterm which achieves mass-renormalization to second order in the fine-structure constant is presented in an appendix.

II. THE MODEL SYSTEM

In this section we discuss briefly the properties of the system under study and the ranges of certain physical parameters which characterize the system. The basic model of the system is discussed in detail in I; here, we simplify that model by neglecting short-range forces and by imposing the high-temperature, low-density limit so that the Coulomb interaction can be neglected. Thus, we are interested in a multicomponent, nonrelativistic fully ionized gas in thermal equilibrium, where the dominant interaction is the transverse electromagnetic interaction between particles and photons.

Since the system is nonrelativistic, thermal energies must be much less than particle rest energies, and photon energies must be insufficient for pair-production; thus, we have the conditions

$$\eta_\alpha \equiv (\beta M_\alpha c^2)^{-1} \ll 1 \tag{2.1}$$

and

$$w_\alpha(\underset{\sim}{k}) \ll w_\gamma(\underset{\sim}{k}) , \tag{2.2}$$

where $\beta \equiv (\kappa T)^{-1}$, κ is the Boltzmann constant, T is the absolute temperature, M_α is the mass of α-type particles and c is the speed of light in vacuo. In Eq. (2.2) we have introduced the particle energy $w_\alpha(\underset{\sim}{k}) = \hbar^2 k^2/2M_\alpha$ and the photon energy $w_\gamma(\underset{\sim}{k}) = \hbar ck$ ($\hbar\underset{\sim}{k}$ is momentum). In the high-temperature, low-density limit the fugacity z_α for α-type particles is given approximately by[2]

$$z_\alpha \equiv \exp(\beta g_\alpha) \simeq \rho_\alpha \lambda_\alpha^3 (2S_\alpha + 1)^{-1} \ll 1 , \tag{2.3}$$

where g_α is the chemical potential (and $g_\gamma = 0$), ρ_α is the number desnity, λ_α is the thermal wavelength, given by

$$\lambda_\alpha = (2\pi\hbar^2\beta/M_\alpha)^{\frac{1}{2}} , \tag{2.4}$$

and S_α is the spin quantum number. The inequality in Eq. (2.3) implies that the average interparticle spacing $\rho_\alpha^{-1/3}$ is much larger than the thermal wavelength λ_α and reflects that in the high-temperature, low-density limit, particle states are weighted statistically by the Boltzmann factor. On the other hand, photon statistics and dynamics are treated entirely quantum mechanically.

The definition of the high-temperature, low-density limit is completed by requiring the Debye length to be much larger than the interparticle spacing; this restriction, with Eq. (2.3), is equivalent to the condition

$$\beta\hbar\,\omega_p \ll 1, \tag{2.5}$$

where the composite plasma frequency ω_p is defined by

$$\omega_p^{\,2} = \sum_\alpha \omega_p^{\,2}(\alpha) = \sum_\alpha 4\pi\rho_\alpha Z_\alpha^{\,2}/M_\alpha , \tag{2.6}$$

$\omega_p(\alpha)$ is the plasma frequency and Z_α the charge number of α-type particles. The inequalities in Eqs. (2.1), (2.2), and (2.5) are mutually compatible for the following temperature and density regions:

$$\left.\begin{array}{l} 0^\circ \ll T < 10^6\ {}^\circ\mathrm{K} \\ \rho \ll 10^{24}\ \text{particles/cm}^3 \end{array}\right\} . \tag{2.7}$$

THE PHOTON SELF-ENERGY

The basic quantities in the generalized master-graph theory of I are the line factors $\mathcal{G}_{\mu,\nu}(t_2,t_1,\underset{\sim}{k}^{\alpha})$ [throughout this paper $\mu + \nu = 2$]. In this section we concentrate on $\mathcal{G}_{1,1}(t_2,t_1,\underset{\sim}{k}^{\gamma})$, defined as the solution of the integral equation, Eq. (I-5.21),[1,9]

$$\mathcal{G}_{1,1}(t_2,t_1,\underset{\sim}{k}^{\gamma}) = \delta(t_2 - t_1) + \int_0^{\beta} ds\, \mathcal{G}_{1,1}(t_2,s,\underset{\sim}{k}^{\gamma})\, Q(s,t_1,\underset{\sim}{k}^{\gamma}) , \tag{3.1}$$

where the kernel $Q(t_2,t_1,\underset{\sim}{k}^{\gamma})$ [Eq. (I-5.20) with $\alpha = \gamma$] is

$$Q(t_2,t_1,\underset{\sim}{k}^{\gamma}) = u_{\gamma}(k)[\Theta(t_2 - t_1) + v'_{\gamma}(\underset{\sim}{k})] + \mathcal{K}_{1,1}(t_2,t_1,\underset{\sim}{k}^{\gamma})$$
$$+ \int_0^{\beta} ds_1 ds_2 \mathcal{K}_{2,0}(t_2,s_1,\underset{\sim}{k}^{\gamma})\, \overline{\mathcal{G}}(s_2,s_1,-\underset{\sim}{k}^{\gamma})\, \mathcal{K}_{0,2}(t_1,s_2,\underset{\sim}{k}^{\gamma}) . \tag{3.2}$$

In Eq. (3.2) $\mathcal{K}_{\mu,\nu}(t_2,t_1,\underset{\sim}{k}^{\gamma})$ is given by the sum of all different generalized master (μ,ν) L-graphs and $\overline{\mathcal{G}}(t_2,t_1,-\underset{\sim}{k}^{\gamma})$ is given by [see Eqs. (I-5.18) and (I-5.19)][10]

$$\overline{\mathcal{G}}(t_2,t_1,-\underset{\sim}{k}^{\gamma}) = \delta(t_2 - t_1) + \int_0^{\beta} ds\, \overline{\mathcal{G}}(t_2,s,-\underset{\sim}{k}^{\gamma})\, \overline{\mathcal{M}}_{1,1}(s,t_1,-\underset{\sim}{k}^{\gamma}) . \tag{3.3}$$

In Eq. (3.3) we have

$$\overline{\mathcal{M}}_{1,1}(t_2,t_1,-\underset{\sim}{k}^{\gamma}) = \overline{u}_{\gamma}(-\underset{\sim}{k})[\Theta(t_2 - t_1) + \overline{v}_{\gamma}(-\underset{\sim}{k})] + \overline{\mathcal{K}}_{1,1}(t_2,t_1,-\underset{\sim}{k}^{\gamma}) , \tag{3.4}$$

where $\overline{\mathcal{K}}_{1,1}(t_2,t_1,-\underset{\sim}{k}^{\gamma})$ is defined diagrammatically analogously to $\mathcal{K}_{1,1}(t_2,t_1,\underset{\sim}{k}^{\gamma})$. Our objective now is to calculate the photon self-energy; to do this we first examine the contributions to the photon counterterm[11] $u_{\gamma}(\underset{\sim}{k})$ in Eq. (3.2) through second order in the fine-structure constant α_0, where $\alpha_0 = e^2/\hbar c$. Thus, as seen from Eqs. (I-2.7) and (I-5.5), this amounts to a renormalization or dressing of the vacuum photon energy $\hbar ck$ to

$$w'_{\gamma}(k) = \hbar ck + u_{\gamma}(k) . \tag{3.5}$$

There are 18 generalized master (μ,ν) graphs of order α_0 and α_0^2, and these are given in Figs. 1 through 4 [the rules for writing down the analytical expressions for generalized master (μ,ν) graphs are given in Appendix A of I]. In order to gain insight into the general <u>structure</u> of the photon self-energy, we must go beyond the diagrams in Figs. 1 through 4 and examine contributions to the second and third terms in Eq. (3.2) which arise from higher-order iterations. Thus, we iterate Eq. (3.3) to obtain

$$\overline{\mathcal{G}}(t_2,t_1,-\underset{\sim}{k}^{\gamma}) = \delta(t_2 - t_1) + \overline{\mathcal{M}}_{1,1}(t_2,t_1,-\underset{\sim}{k}^{\gamma}) + \int_0^{\beta} ds\, \overline{\mathcal{M}}_{1,1}(t_2,s,-\underset{\sim}{k}^{\gamma})\, \overline{\mathcal{M}}_{1,1}(s,t_1,-\underset{\sim}{k}^{\gamma}) + \cdots, \tag{3.6}$$

where $\overline{\mathcal{M}}_{1,1}(t_2,t_1,-\underset{\sim}{k}^{\gamma})$ is defined in Eq. (3.4). We use Eq. (3.6) and rewrite Eq. (3.2) in the iterated form

$$Q(t_2,t_1,\underset{\sim}{k}^{\gamma}) = u_{\gamma}(\underset{\sim}{k})[\theta(t_2 - t_1) + v'_{\gamma}(\underset{\sim}{k})] + \sum_i \mathcal{K}^{(i)}_{1,1}(t_2,t_1,\underset{\sim}{k}^{\gamma})$$

$$+ \int_0^{\beta} ds_1 ds_2 \left\{ \left[\sum_j \mathcal{K}^{(j)}_{2,0}(t_2,s_1,\underset{\sim}{k}^{\gamma}) \right] \left[\delta(s_2 - s_1) + \overline{\mathcal{M}}_{1,1}(s_2,s_1,-\underset{\sim}{k}^{\gamma}) \right.\right.$$

$$\left.\left. + \int_0^{\beta} ds\, \overline{\mathcal{M}}_{1,1}(s_2,s,-\underset{\sim}{k}^{\gamma})\, \overline{\mathcal{M}}_{1,1}(s,s_1,-\underset{\sim}{k}^{\gamma}) + \cdots \right] \left[\sum_{\ell} \mathcal{K}^{(\ell)}_{0,2}(t_1,s_2,\underset{\sim}{k}^{\gamma}) \right] \right\}. \tag{3.7}$$

In this paper we discuss explicitly the iterations which arise from the graphs in Figs. 1 through 4; thus, in Eq. (3.7), i runs over the 14 graphs in Figs. 1 through 3, j runs over the two (2,0) graphs in Fig. 4, ℓ runs over the two (0,2) graphs in Fig. 4 and $\overline{\mathcal{M}}_{1,1}(t_2,t_1,-\underset{\sim}{k}^{\gamma})$ will be approximated by $\overline{\mathcal{M}}^{(2)}_{1,1}(t_2,t_1,-\underset{\sim}{k}^{\gamma})$ [see Eq. (3.4) and the second graph in Fig. 1], since $\overline{\mathcal{M}}^{(1)}_{1,1}(t_2,t_1,-\underset{\sim}{k}^{\gamma}) \simeq 0$ [see Eq. (3.18), below]. Next, it is convenient to separate $u_{\gamma}(\underset{\sim}{k})$ into two parts

$$u_{\gamma}(\underset{\sim}{k}) = u_{\gamma}(\underset{\sim}{k})_1 + u'_{\gamma}(\underset{\sim}{k}) , \tag{3.8}$$

where $u_{\gamma}(\underset{\sim}{k})_1$ is the contribution to $u_{\gamma}(\underset{\sim}{k})$ from (1,1) graphs [the first sum in Eq. (3.7)], and $u'_{\gamma}(\underset{\sim}{k})$ is the remaining contribution which involves the (2,0) and (0,2) graphs [arising from the sums over j and ℓ in Eq. (3.7)].

It is straightforward to write down the analytic expression for $\mathcal{K}^{(i)}_{1,1}(t_2,t_1,\underset{\sim}{k}^{\gamma})$, $i=1,2,\cdots,14$, in Eq. (3.7) and then to identify the corresponding self-energies $u_{\gamma}^{(i)}(\underset{\sim}{k})$.[8] Here, for the sake of

illustration, we give the approximate expressions for the two graphs in Fig. 1. We use

$$\mathcal{G}_{1,1}(t_2,t_1,\underset{\sim}{k}^{\alpha}) \simeq \delta(t_2 - t_1) , \tag{3.9}$$

the lowest order approximation to the particle line factor in Eq. (I-5.21), to obtain, assuming mass-renormalization has been performed (see the Appendix),[12,13]

$$\mathcal{K}^{(1)}_{1,1}(t_2,t_1,\underset{\sim}{k}^{\gamma})$$

$$\simeq - \frac{2\pi\hbar^2\alpha_0}{\Omega k} \sum_{\alpha} Z_{\alpha}^{2}(2S_{\alpha} + 1)M_{\alpha}^{-1} \sum_{\underset{\sim}{k}_1} \nu_{\alpha}(\underset{\sim}{k}_1)[\theta(t_2 - t_1) + \nu'_{\gamma}(k)] , \tag{3.10}$$

$$\mathcal{K}^{(2)}_{1,1}(t_2,t_1,\underset{\sim}{k}^{\gamma})$$

$$\simeq \frac{2\pi\hbar^4\alpha_0}{\Omega k} \sum_{\alpha} Z_{\alpha}^{2}(2S_{\alpha} + 1)M_{\alpha}^{-2} \sum_{\underset{\sim}{k}_1,\underset{\sim}{k}_2} (\underset{\sim}{k}_2 \cdot \hat{e}_{\underset{\sim}{k}})^2 W_1^{-1} \delta_{\underset{\sim}{k}_1,(\underset{\sim}{k}_2+\underset{\sim}{k})}$$

$$\times [\nu_{\alpha}(\underset{\sim}{k}_2) - \nu_{\alpha}(\underset{\sim}{k}_1)][\theta(t_2 - t_1) + \nu'_{\gamma}(\underset{\sim}{k})] + F(t_2,t_1,\underset{\sim}{k}^{\gamma}) , \tag{3.11}$$

where

$$F(t_2,t_1,\underset{\sim}{k}^{\gamma})$$

$$= - \frac{2\pi\hbar^4\alpha_0}{\Omega k} \sum_{\alpha} Z_{\alpha}^{2}(2S_{\alpha} + 1)M_{\alpha}^{-2} \sum_{\underset{\sim}{k}_1,\underset{\sim}{k}_2} (\underset{\sim}{k}_2 \cdot \hat{e}_{\underset{\sim}{k}})^2 W_1^{-1} \delta_{\underset{\sim}{k}_1,(\underset{\sim}{k}_2+\underset{\sim}{k})}$$

$$\times [\theta(t_2 - t_1)\nu_{\alpha}(\underset{\sim}{k}_2) + \theta(t_1 - t_2)\nu_{\alpha}(\underset{\sim}{k}_1) + \epsilon_{\alpha}\nu_{\alpha}(\underset{\sim}{k}_1)\nu_{\alpha}(\underset{\sim}{k}_2)]$$

$$\times \exp[(t_1 - t_2)W_1] , \tag{3.12}$$

$$W_1 = w_\alpha(\underset{\sim}{k}_1) - w_\alpha(\underset{\sim}{k}_2) - w'_\gamma(\underset{\sim}{k}) , \tag{3.13}$$

$$\nu'_\gamma(\underset{\sim}{k}) = \left[e^{\beta w'_\gamma(k)} - 1\right]^{-1} , \tag{3.14}$$

$$\nu_\alpha(\underset{\sim}{k}) = \left\{e^{\beta[w_\alpha(k)-g_\alpha]} - \epsilon_\alpha\right\}^{-1} , \tag{3.15}$$

$\epsilon_\alpha = +1$ for α = boson, $\epsilon_\alpha = -1$ for α = fermion and $\hat{e}_{\underset{\sim}{k}}$ is the photon unit polarization vector (as in I, we are using the Coulomb gauge). In the high-temperature, low-density limit as expressed by Eq. (2.3) and with the nonrelativistic condition in Eq. (2.2), we have from Eqs. (3.10) and (3.11) the approximate photon self-energy contributions[11]

$$u_\gamma^{(1)}(\underset{\sim}{k})_1 \simeq \hbar^2 \omega_p^2/2\hbar ck , \tag{3.16}$$

$$u_\gamma^{(2)}(\underset{\sim}{k})_1 \simeq -16\pi^2 \hbar^2 \alpha_0 k^{-3} \sum_\alpha \rho_\alpha Z_\alpha^2 M_\alpha^{-1} \lambda_\alpha^{-2} \frac{[w_\alpha(k)]^2}{[w'_\gamma(k)]^2 - [w_\alpha(k)]^2} . \tag{3.17}$$

Here, we see that the choice in Eq. (3.16) leads to the result

$$\overline{\mathcal{M}}_{1,1}^{(1)}(t_2,t_1,-\underset{\sim}{k}^\gamma) \simeq \mathcal{M}_{1,1}^{(1)}(t_2,t_1,\underset{\sim}{k}^\gamma) \simeq 0 . \tag{3.18}$$

Once the mass-renormalization counterterm has been introduced, a straightforward, but tedious, calculation leads to the conclusions

$$\sum_{i=3}^{14} u_\gamma^{(i)}(k)_1 \ll u_\gamma^{(2)}(k)_1 \ll u_\gamma^{(1)}(k) . \tag{3.19}$$

Thus, the contributions $u_\gamma^{(i)}(k)_1$, $i=3,\cdots,14$, can be neglected.

Now, we examine the contributions to $u'_\gamma(\underset{\sim}{k})$ which arise from the temperature independent parts of $\int ds\, \mathcal{K}^{(j)}_{2,0}\, \bar{\mathcal{G}}\, \mathcal{K}^{(\ell)}_{0,2}$ in Eq. (3.7). To do this, it is useful to simplify the notation; thus, corresponding to the appropriate terms in Eq. (3.7), we identify symbolically the following <u>temperature independent</u> quantities:[11]

$$u'_\gamma(\underset{\sim}{k}) = \sum_{j,\ell,p,r,\ldots} u'_\gamma(\underset{\sim}{k})_{j\ell pr\ldots} , \tag{3.20}$$

where, in simplified notation,

$$u'_\gamma(\underset{\sim}{k})_{j\ell pr\ldots} = -\left\{\int_0^\beta ds_1 ds_2\, \mathcal{K}^{(j)}_{2,0}(s_1)\, \mathcal{K}^{(\ell)}_{0,2}(s_2)\right.$$

$$\left. \times \left[\delta(s_2 - s_1) + \bar{\mathcal{M}}^{(p)}_{1,1}(s_2,s_1) + \int_0^\beta ds\, \bar{\mathcal{M}}^{(p)}_{1,1}(s_2,s)\bar{\mathcal{M}}^{(r)}_{1,1}(s,s_1) + \cdots\right]\right\}_{\text{T.I.P.}} , \tag{3.21}$$

and T.I.P. denotes temperature-independent part. In what follows, we examine Eq. (3.21) with $p = r = 2$ [recall Eq. (3.18)], and the p and r subscripts used in Eq. (3.20) will be suppressed.

Next, we attempt to discover the general structure of $u_\gamma(k)$; in order to do this, we start with a detailed examination of the three leading order contributions to Eq. (3.20) given in Figs. 5 through 7. We find after some tedious manipulations,[14]

$$u'_\gamma(k)_{11} = -[u_\gamma^{(1)}(k)_1]^2\, W^{-1}(1 - R)^{-1} , \tag{3.22}$$

$$u'_\gamma(k)_{12} = u'_\gamma(k)_{21} \tag{3.23}$$

$$= -[u_\gamma^{(1)}(k)_1\, u_\gamma^{(2)}(k)_1]W^{-1}(1 - R)^{-1} , \tag{3.24}$$

where

$$R = 2\pi\, \hbar^4 \alpha_0 \Omega^{-1} k^{-1} \sum_\alpha Z_\alpha^{\,2}(2S_\alpha + 1)\, M_\alpha^{\,-2} \sum_{\underset{\sim}{k}_1, \underset{\sim}{k}_2} (\underset{\sim}{k}_1 \cdot \hat{e}_{\underset{\sim}{k}})^2\, \delta_{\underset{\sim}{k}_1, (\underset{\sim}{k}_2 - \underset{\sim}{k})}$$

$$\times\ [\nu_\alpha(\underset{\sim}{k}_1) - \nu_\alpha(\underset{\sim}{k}_2)]\, \overline{W}_1^{\,-1}\, W_4^{\,-1}, \tag{3.25}$$

$$W = w'_\gamma(\underset{\sim}{k}) + \overline{w}_\gamma(-\underset{\sim}{k}) , \tag{3.26}$$

$$\begin{aligned} W_4 &= w_\alpha(\underset{\sim}{k}_1) - w_\alpha(\underset{\sim}{k}_2) + w'_\gamma(\underset{\sim}{k}) \\ \overline{W}_1 &= w_\alpha(\underset{\sim}{k}_1) - w_\alpha(\underset{\sim}{k}_2) - \overline{w}_\gamma(-\underset{\sim}{k}) \end{aligned} \tag{3.27}$$

and W_1 is given in Eq. (3.13). The important point here is that temperature integrals and momentum sums have decoupled in such a way as to enable factorization of terms in Eq. (3.21) and the summation of the resultant geometric series. With the results in Eqs. (3.22)-(3.24), we obtain for Eq. (3.20)

$$u'_\gamma(k) \simeq -[u_\gamma^{(1)}(\underset{\sim}{k})_1 + u_\gamma^{(2)}(\underset{\sim}{k})_1]^2\, W^{-1}(1 - R)^{-1} . \tag{3.28}$$

We have examined Eq. (3.20) for all combinations of the graphs in Figs. 1 through 4 (as well as for a few more complicated graphical structures) and have obtained the more general result

$$u'_\gamma(\underset{\sim}{k}) = [u_\gamma(\underset{\sim}{k})_1]^2\, W^{-1}\{[\overline{u}_\gamma(-\underset{\sim}{k})_1 - \tilde{u}_\gamma(\underset{\sim}{k})_1]W^{-1} - 1\}^{-1} , \tag{3.29}$$

where $\tilde{u}_\gamma(\underset{\sim}{k})_1$ is to be obtained from $u_\gamma(\underset{\sim}{k})_1$ by changing $\underset{\sim}{k}$ to $-\underset{\sim}{k}$ and then replacing $w'_\gamma(-\underset{\sim}{k})$ by $-w'_\gamma(\underset{\sim}{k})$ wherever this quantity occurs inside momentum sums. Now, we introduce[15]

$$w'_\gamma(\underset{\sim}{k}) \equiv \hbar ck + u_\gamma(\underset{\sim}{k})_1 + u'_\gamma(\underset{\sim}{k}) \equiv w'_\gamma(\underset{\sim}{k})_1 + u'_\gamma(\underset{\sim}{k}) , \tag{3.30}$$

$$\bar{w}_\gamma(-\underset{\sim}{k}) \equiv \hbar ck + \bar{u}_\gamma(-\underset{\sim}{k})_1 , \tag{3.31}$$

$$\tilde{w}_\gamma(\underset{\sim}{k})_1 \equiv \hbar ck + \tilde{u}_\gamma(\underset{\sim}{k})_1 , \tag{3.32}$$

and use Eq. (3.29) to rewrite Eq. (3.8) in the form

$$w'_\gamma(\underset{\sim}{k}) = w'_\gamma(\underset{\sim}{k})_1 - [u_\gamma(\underset{\sim}{k})_1]^2 [w'_\gamma(\underset{\sim}{k}) + \tilde{w}_\gamma(\underset{\sim}{k})_1]^{-1} , \tag{3.33}$$

which, in turn, can be solved for $w'_\gamma(\underset{\sim}{k})$ to give

$$w'_\gamma(\underset{\sim}{k}) = \frac{1}{2} [u_\gamma(\underset{\sim}{k})_1 - \tilde{u}_\gamma(\underset{\sim}{k})_1] + \frac{1}{2}\{[w'_\gamma(\underset{\sim}{k})_1 + \tilde{w}_\gamma(\underset{\sim}{k})_1]^2 - 4[u_\gamma(\underset{\sim}{k})_1]^2\}^{\frac{1}{2}} . \tag{3.34}$$

Here, it is to be realized that the simple form of Eq. (3.34) is deceptive, since it is actually a nonlinear integral equation.

We suggest that Eq. (3.26) and, hence, Eq. (3.32) are formally exact. Of course, this assertion is based only on the experience gained by the detailed examination of the perturbation series in Eqs. (3.7) and (3.21) with the approximation given in Eq. (3.9). Also, we note that the inclusion of the Coulomb interaction would not alter the procedures used above. A general proof of this assertion, if one exists, has not yet been developed. The main question is whether energy denominators occurring in Eq. (3.21) can be factorized (to give decoupling).

For the 14 graphs in Figs. 1 through 3, relabelling leads to the result

$$u_\gamma(\underset{\sim}{k})_1 - \tilde{u}_\gamma(\underset{\sim}{k})_1 \simeq \sum_{i=1}^{14} [u_\gamma^{(i)}(\underset{\sim}{k})_1 - \tilde{u}_\gamma^{(i)}(\underset{\sim}{k})_1] = 0 . \tag{3.35}$$

Moreover, using Eq. (3.19) and the analogous relation for $\tilde{u}_\gamma^{(i)}(\underset{\sim}{k})$ and assuming the high-temperature, low-density limit, we have for Eq. (3.34)

$$w'_\gamma(\underset{\sim}{k}) \simeq [(\hbar ck)^2 + \hbar^2\omega_p^{\,2} + 2\hbar ck\, u_\gamma^{(2)}(\underset{\sim}{k})_1]^{\frac{1}{2}} , \tag{3.36}$$

where $u_\gamma^{(2)}(\underset{\sim}{k})_1$ is given by Eq. (3.17), and Eqs. (3.16) and (3.35) have been used. In fact, Eq. (3.36) is given, to a good approximation, by

$$w'_\gamma(\underset{\sim}{k}) \simeq [(\hbar ck)^2 + \hbar^2\, \omega_p^{\,2}]^{\frac{1}{2}} \equiv w_\Gamma(\underset{\sim}{k}) , \tag{3.37}$$

because, for all k, $\left|2\hbar ck\, u_\gamma^{(2)}(\underset{\sim}{k})_1 [w_\Gamma(\underset{\sim}{k})]^{-2}\right|$ is bounded by $(2\omega_p^{\,2})^{-1} \sum_\alpha \eta_\alpha\, \omega_p^{\,2}(\alpha)$ which is always small, since $\omega_p^{\,2} \geq \omega_p^{\,2}(\alpha)$ and $\eta_\alpha \ll 1$ [see Eq. (2.1)]. Thus, in conclusion, Eq. (3.37) represents accurately the photon self-energy (in the high-temperature, low-density limit).

It is interesing to note that the photon self-energy in Eq. (3.37) corresponds precisely to that obtained in the pair-Hamiltonian approximation, which is diagrammatically equivalent to considering only the two graphs in Fig. 8. Moreover, as will be indicated in Sec. IV, the pair-Hamiltonian can be diagonalized by a Bogoliubov transformation,[16] and the resulting quasi-photon energy is that given by Eq. (3.37). The dominant nature of Eq. (3.37) as an

approximation to $w'_\gamma(\underset{\sim}{k})$ in Eq. (3.34) suggests that the pair-Hamiltonian is a good starting point for a perturbation theoretic development - this point of view will be adopted henceforth. At the end of the following section, the pair-Hamiltonian and the Bogoliubov transformation are discussed in detail.

IV. THE PHOTON MOMENTUM DISTRIBUTION

In this section we calculate the photon momentum distribution $\langle n_\gamma(\underset{\sim}{k})\rangle$ [which is the average number of photons with momentum $\underset{\sim}{k}$ -- see Eq. (4.16), below]. Thus, we are to evaluate [see Eqs. (I-3.7) and (I-5.24)]

$$\langle n_\gamma(\underset{\sim}{k})\rangle = \nu'_\gamma(k)\int_0^\beta ds\ \mathcal{G}_{1,1}(\beta,s,\underset{\sim}{k}^\gamma) , \tag{4.1}$$

where $\nu'_\gamma(\underset{\sim}{k})$ is given in Eq. (3.14), and the line factor $\mathcal{G}_{1,1}(t_2,t_1,\underset{\sim}{k}^\gamma)$ is given by Eq. (3.1). The choice of counterterms made in the preceding section leads to the cancellation of all temperature independent parts of Eq. (3.2), so that the kernel $Q(t_2,t_1,\underset{\sim}{k}^\gamma)$ in Eqs. (3.1) and (3.2) involves now only temperature dependent parts (T.D.P.).[11]

First, we observe that the vertex functions for the electromagnetic interactions [Eqs. (I-5.2) - (I-5.6) give rise to factors of $1/k$ in Eq. (3.2) so that the iterative solution of Eq. (3.1) is not valid for $k \to 0$; thus, we should always seek noniterative solutions of Eq. (3.1). It is easy to find the exact, noniterative solution of Eq. (3.1) in the pair-Hamiltonian approximation (which corresponds to the two graphs in Fig. 8). However, since the contributions of the (2,0) and (0,2) photon self-energy structures are of particular interest, we go beyond the simple pair-Hamiltonian approximation and include the leading order contributions to $\mathcal{G}_{1,1}(t_2,t_1,\underset{\sim}{k}^\gamma)$ which arise from these structures. Thus, instead of the graphs in Fig. 8, we examine those

in Fig. 9. Corresponding to the diagrams in Fig. 9 and for the selection of counterterms made in the preceding section, the kernel in Eq. (3.2) is

$$Q(t_2,t_1,\underset{\sim}{k}^{\gamma}) \simeq [\Theta(t_1 - t_2) + \bar{\nu}_{\gamma}(-\underset{\sim}{k})]E \ \exp[(t_1 - t_2)W] , \tag{4.2}$$

where

$$E = [\bar{u}_{\gamma}^{(1)}(-\underset{\sim}{k})_1 + \bar{u}_{\gamma}^{(2)}(-\underset{\sim}{k})_1]^2 \ W^{-1} \tag{4.3}$$

and W is given in Eq. (3.26). Now, with Eq. (4.2), the line factor in Eq. (3.1) is obtained by solving the integral equation

$$\mathcal{G}'_{1,1}(t_2,t_1,\underset{\sim}{k}^{\gamma}) \simeq \delta(t_2 - t_1) + \int_0^{\beta} ds \, \mathcal{G}'_{1,1}(t_2,s,\underset{\sim}{k}^{\gamma})E$$

$$\times \ [\Theta(t_1 - s) + \bar{\nu}_{\gamma}(-\underset{\sim}{k})] \exp[(s - t_1)W] . \tag{4.4}$$

In the high-temperature, low-density limit $\bar{u}_{\gamma}^{(1)}(-\underset{\sim}{k})_1$ is given approximately by Eq. (3.16) and $\bar{u}_{\gamma}^{(2)}(-\underset{\sim}{k})_1$ by Eq. (3.17); thus, in this case, the kernel of Eq. (4.4) diverges for $k \to 0$. This causes no problem since the exact, noniterative solution to Eq. (4.4) is found to be

$$\mathcal{G}'_{1,1}(t_2,t_1,\underset{\sim}{k}^{\gamma}) = \delta(t_2 - t_1) + E[\Theta(t_1 - t_2) + M]$$

$$\times \ \exp[(t_2 - t_1)(W - E)] , \tag{4.5}$$

where

$$M^{-1} = \exp(-\beta E)\ \{1 + [\bar{\nu}_\gamma(-\underset{\sim}{k})]^{-1}\} - 1 \ . \tag{4.6}$$

Next, we use Eq. (4.5) as an approximate solution to Eq. (3.1) and introduce the lowest order temperature dependent contribution of the diagrams in Figs. 1 through 3, namely that from the second diagram in Fig. 1. Thus, to this order, we obtain

$$\mathcal{G}_{1,1}(t_2,t_1,\underset{\sim}{k}^\gamma) \simeq \mathcal{G}'_{1,1}(t_2,t_1,\underset{\sim}{k}^\gamma) + F(t_2,t_1,\underset{\sim}{k}^\gamma) \ , \tag{4.7}$$

where $F(t_2,t_1,\underset{\sim}{k}^\gamma)$ is given by Eq. (3.12). Since Eq. (3.12) has a factor of k^{-1}, Eq. (4.7) can not be used to construct an iterative solution of Eq. (3.1) for small k. Analogous to the procedures used in the preceding section, we have developed a partial summation program to obtain solutions to Eq. (3.1) which cause no problem for small k. However, the resulting analytical expressions are not particularly illuminating and are perhaps not useful, since it is difficult to assess the relative importance of neglected terms in the integral equation. With these points in mind, we use Eq. (4.7) to estimate the photon momentum distribution in Eq. (4.1). In the high-temperature, low-density limit we obtain for Eq. (4.1) with Eq. (4.7)

$$\begin{aligned}\langle n_\gamma(\underset{\sim}{k})\rangle &\simeq \nu'_\gamma(\underset{\sim}{k}) + \nu'_\gamma(\underset{\sim}{k})\ EM(W - E)^{-1}\ \{\exp[\beta(W - E)] - 1\} \\ &+ (2\beta\hbar ck)^{-1} \sum_\alpha \hbar^2\omega_p{}^2(\alpha)\ [w'_\gamma(\underset{\sim}{k}) + w_\alpha(\underset{\sim}{k})]^{-2} \ .\end{aligned} \tag{4.8}$$

We wish to explore the meaning of this result, by examining its lowest-order approximation; thus, we use Eq. (3.19), Eq. (3.16) for $\bar{u}_\gamma{}^{(1)}(-\underset{\sim}{k})_1$ and Eq. (3.37) for $w'_\gamma(\underset{\sim}{k})$ to obtain[17]

$$\langle n_\gamma(\underset{\sim}{k})\rangle \simeq [f_-(\underset{\sim}{k})]^2 + \{[f_+(\underset{\sim}{k})]^2 + [f_-(\underset{\sim}{k})]^2\}\, \nu_\Gamma(\underset{\sim}{k})$$

$$+ (2\beta\hbar ck)^{-1} \sum_\alpha \hbar^2 \omega_p{}^2(\alpha)[w_\Gamma(\underset{\sim}{k}) + w_\alpha(\underset{\sim}{k})]^{-2}, \tag{4.9}$$

where

$$[f_+(\underset{\sim}{k})]^2 - [f_-(\underset{\sim}{k})]^2 = 1 \tag{4.10}$$

$$[f_+(\underset{\sim}{k})]^2 = [w_\Gamma(\underset{\sim}{k}) + \bar{w}_\gamma{}^{(1)}(-\underset{\sim}{k})][2w_\Gamma(\underset{\sim}{k})]^{-1} \tag{4.11}$$

$$\nu_\Gamma(\underset{\sim}{k}) = \{\exp[\beta w_\Gamma(\underset{\sim}{k})] - 1\}^{-1} \tag{4.12}$$

with $\bar{w}_\gamma{}^{(1)}(-\underset{\sim}{k}) = \hbar ck + \bar{u}_\gamma{}^{(1)}(-\underset{\sim}{k})_1$. We see that Eqs. (4.8) and (4.13) diverge as k^{-1} for small k; this same divergence is also exhibited by the Planck or free-photon distribution function. However, this kind of behavior is of no consequence, since in calculations of all measurable quantities the divergence is removed by the density-of-states factor. Thus, in lowest order, we have obtained a result which does not suffer from the infrared divergence. It is interesting to note that the first term in Eq. (4.9) is independent of the system temperature; the electrodynamic origin of this term is not clear.

In closing this section we wish to indicate the connection between Eqs. (3.37), (4.9), and the pair-Hamiltonian, H_p. It is straightforward to extract H_p from the system Hamiltonian;[16] the result is

$$H_p = \sum_{\underset{\sim}{k}} \{(\hbar ck + \hbar^2 \omega_p^{\,2}/2\hbar ck)\, a^\dagger(\underset{\sim}{k})\, a(\underset{\sim}{k})$$

$$+ \hbar^2 \omega_p^{\,2} (2\hbar ck)^{-1} [a^\dagger(\underset{\sim}{k})\, a^\dagger(-\underset{\sim}{k}) + a(\underset{\sim}{k})\, a(-\underset{\sim}{k})]\} , \qquad (4.13)$$

where $a^\dagger(\underset{\sim}{k})$ and $a(\underset{\sim}{k})$ are photon creation and annihilation operators. The pair-Hamiltonian can be diagonalized by means of a Bogoliubov transformation; thus, one introduces the quasi-photon creation and annihilation operators $b^\dagger(\underset{\sim}{k})$ and $b(\underset{\sim}{k})$ as follows:

$$\begin{aligned} a^\dagger(\underset{\sim}{k}) \rightarrow U\, a^\dagger(\underset{\sim}{k}) U^\dagger &\equiv f_+(\underset{\sim}{k})\, b^\dagger(\underset{\sim}{k}) - f_-(\underset{\sim}{k})\, b(-\underset{\sim}{k}) , \\ a(\underset{\sim}{k}) \rightarrow U\, a(\underset{\sim}{k}) U^\dagger &\equiv f_+(\underset{\sim}{k})\, b(\underset{\sim}{k}) - f_-(\underset{\sim}{k})\, b^\dagger(-\underset{\sim}{k}) , \end{aligned} \qquad (4.14)$$

where $f_+(\underset{\sim}{k})$ and $f_-(\underset{\sim}{k})$ are given by Eqs. (4.10)-(4.12). One readily verifies that

$$H_p' = U\, H_p\, U^\dagger = \sum_{\underset{\sim}{k}} w_\Gamma(\underset{\sim}{k})\, b^\dagger(\underset{\sim}{k})\, b(\underset{\sim}{k}) , \qquad (4.15)$$

where $w_\Gamma(\underset{\sim}{k})$ is given in Eq. (3.37). Now, we can also relate the <u>true photon</u> momentum distribution and the <u>quasi-photon</u> momentum distribution. If we introduce the transformation in Eq. (4.14) into the definition of the photon momentum distribution, namely

$$\langle n_\gamma(\underset{\sim}{k}) \rangle \equiv \mathrm{Tr}[\rho\, a^\dagger(\underset{\sim}{k})\, a(\underset{\sim}{k})] , \qquad (4.16)$$

we obtain

$$\langle n_\gamma(\underset{\sim}{k})\rangle = [f_-(\underset{\sim}{k})^2 + \{[f_+(\underset{\sim}{k})]^2 + [f_-(\underset{\sim}{k})]^2\}\, \mathrm{Tr}[\rho'\, b^\dagger(\underset{\sim}{k})\, b(\underset{\sim}{k})]$$

$$- f_-(\underset{\sim}{k})\, f_+(\underset{\sim}{k})\, \mathrm{Tr}\{\rho'[b^\dagger(\underset{\sim}{k})\, b^\dagger(-\underset{\sim}{k}) + b(\underset{\sim}{k})\, b(-\underset{\sim}{k})]\} \; . \qquad (4.17)$$

In Eq. (4.16) ρ is the density operator for the grand canonical ensemble, and in Eq. (4.17)

$$\rho' = U\rho U^\dagger \; . \qquad (4.18)$$

One observes that $\mathrm{Tr}[\rho'\, b^\dagger(\underset{\sim}{k})\, b(\underset{\sim}{k})]$ is the quasi-photon momentum distribution. The quasi-photon momentum distribution has been calculated earlier (for the two diagrams in Fig. 1, as well as for a Coulomb correction),[6] and, on the basis of Eq. (4.17), the result is in accord with our lowest-order results for the true photon momentum distribution.

We see that Eq.(4.17) is, in lowest-order, equivalent to Eq. (4.9); this suggests that the pair-Hamiltonian is a useful choice of unperturbed Hamiltonian for a perturbation theory of interacting radiation and charges.[18] Moreover, Eq.(4.17) provides the formal relation between the photon and quasi-photon momentum distributions; however, this relation is not as useful as it may appear, since it is now necessary to construct a calculational scheme for evaluating the last two terms in Eq. (4.17) [note that these terms are inherently (2,0) and (0,2) structures]. Finally, we observe that the infrared divergence does not occur in the quasi-photon representation;[16] thus, in Eq. (4.17), the infrared divergence has been relegated completely to the factors involving $f_+(\underset{\sim}{k})$ and $f_-(\underset{\sim}{k})$.

V. DISCUSSION

A principal goal of this investigation was to determine the importance of the complete photon self-energy analysis on the calculations of the properties of photons in a fully-ionized gas. The most interesting result of this study is the photon energy-momentum relation given in Eq.(3.34), and we note that the form of this expression is determined primarily by the analysis of the (2,0) and (0,2) photon structures; thus, these structures, which have not been included completely in any of the prior investigations,[3-7] play a very significant role in determining the dressed photon energy.

The expression for the momentum distribution in Eq. (4.8) also has certain features not observed before, since earlier calculations[3-7] did not include the self-energy analysis of (2,0) and (0,2) structures and since some of these calculations[6,7] were for the quasi-photon momentum distribution. It is recalled that the noniterative result in Eq. (4.5) was important in determining the result in Eq. (4.8). At this point, we remark that a complete understanding of the properties of photons in an interacting system (as considered herein) cannot be based solely on the quantities which we have investigated, and additional functions must be determined. In particular, knowledge of the dynamic structure factor is of extreme value, since this can be used to understand the modes of propagation of photons and also the related lifetimes.

In Sec. IV we have indicated that in the photon momentum distribution the infrared divergence can be extracted by means of a

Bogoliubov transformation, but that it will be difficult to calculate the resulting expression. Since the infrared divergence is of electrodynamic origin, it would be more pleasing to analyze this problem on a more fundamental level. Thus, we are currently pursuing the infrared problem, along the lines initiated by Kibble,[19] by using a nonseparable Hilbert space for describing photon states.

As a result of this investigation, we conclude that the new formalism in I, in addition to performing a complete self-energy analysis, is much simpler in practice than its predecessor.[2] As a direct outcome of the simplifications introduced by the new formalism, it has been possible to sum certain important infinite series to all orders. Another important feature of the theory in I is the counterterm technique. It is apparent that the technique is particularly well-suited for investigating the self-energy properties associated with single particles or photons (as opposed to collective excitations); examples of this type of self-energy problem are provided by mass-renormalization, the dressed photon energy and the one-particle problem of MG.[20] The Coulomb and infrared divergences seem to be less susceptible to a direct application of the counterterm technique.

The connections between the line factors in I and single-particle Green functions have been established recently.[21] Thus, starting with the line-factors in Sec. IV, we could now calculate the normal and anomalous single-particle Green functions for the equilibrium fully ionized gas -- such calculations have not yet been performed. However, in the present paper, we have observed consistently the $(t_2 - t_1)$-temperature dependence established in the Green function theory.[21]

ACKNOWLEDGMENTS

The authors would like to thank Professors Geoffrey Chew and Kenneth Watson for extending the hospitality of the Lawrence Radiation Laboratory at Berkeley. One of us (C.R.S.) wishes to thank Associated Western Universities, Inc., for the faculty fellowship at Lawrence Radiation Laboratory. Finally, we express our appreciation to Professor Franz Mohling and Dr. I. RamaRao for illuminating discussions.

APPENDIX

In the calculations of this paper no use is made of the explicit expressions for the (1,1) graphs of order α_0^2 in Figs. 2 and 3, since (after mass renormalization) they are much smaller than the other contributions which are taken into account. On the other hand, if the expressions for the graphs in Fig. 2 are examined, it is found that (before mass renormalization) these expressions diverge for large photon momentum - this is a manifestation of the ultraviolet divergence of quantum electrodynamics. The need for mass renormalization occurs because in the Hamiltonian the electromagnetic field associated with each charged particle is separated from the particle so that bare particles interact with the total electromagnetic field. Since it is meaningless from an experimental standpoint to separate a charged particle and its associated field, it is clear that the separation mentioned above must be a mathematical convenience and can be of no further consequence. The mass-renormalization technique developed in I is designed to replace bare-particle masses by their experimentally observed masses. Below, we outline how mass renormalization is used to cancel the ultraviolet divergences in the graphs in Fig. 2 to obtain the finite contributions from these graphs.

The mass-renormalization procedure developed in I is quite straightforward; however, since some skill may be involved in applying the technique, we now indicate how one approaches the selection of the mass-renormalization counterterm. Thus, following I, we combine the kinetic energy of the bare particle

$$w_\alpha^{(0)}(k) = \hbar^2 k^2/2M_\alpha^{(0)} \tag{A.1}$$

and the mass-renormalization counterterm

$$S_\alpha(k) = (\hbar^2 k^2/2M_\alpha)D_\alpha \tag{A.2}$$

so as to achieve the correct single-particle kinetic energy:

$$w_\alpha(k) = w_\alpha^{(0)}(k) + S_\alpha(k) = \hbar^2 k^2/2M_\alpha \ . \tag{A.3}$$

Above, $M_\alpha^{(0)}$ is the bare mass, M_α is the observed mass and

$$1/M_\alpha^{(0)} \equiv (1 - D_\alpha)/M_\alpha \ . \tag{A.4}$$

As noted earlier,[5] the kinetic energy in Eq. (A.3) is to be quadratic in k so that D_α must be independent of k. Then, the identity in Eq. (A.4) is used to re-express the bare masses in the interaction vertices in terms of M_α and D_α, which in turn determine $S_\alpha(k)$.

Next, we combine the diagrams in Figs. 1 and 2 as follows:

$$\mathcal{K}_{1,1}^{(1)} + \mathcal{K}_{1,1}^{(3)} + \mathcal{K}_{1,1}^{(4)} \tag{A.5}$$

$$\mathcal{K}_{1,1}^{(2)} + \mathcal{K}_{1,1}^{(5)} + \cdots + \mathcal{K}_{1,1}^{(8)} \ . \tag{A.6}$$

By relabelling, one can extract a factor $\mathcal{K}_{1,1}^{(1)}$ in Eq. (A.5) and a factor $\mathcal{K}_{1,1}^{(2)}$ in Eq. (A.6); in the remaining factors in Eqs. (A.5) and (A.6) it is possible to select the quantity D_α to cancel the ultraviolet divergences in these terms. We state the result:

$$D_\alpha = (4\pi\alpha_0\hbar^2 Z_\alpha{}^2/M_\alpha\Omega) \sum_{\underset{\sim}{k}_4} (\hat{e}_{\underset{\sim}{k}} \cdot \hat{e}_4)^2 \, k_4{}^{-1} [w_\alpha(\underset{\sim}{k}_4) + w'_\gamma(\underset{\sim}{k}_4)]^{-1} \, . \tag{A.7}$$

This defines a counterterm, Eq. (A.2), which cancels, through order $\alpha_0{}^2$, the ultraviolet divergences everywhere in the theory. In order to obtain Eq. (A.7) the following identities (relating to the angular integrations) are useful:

$$\int_{-1}^{1} d\mu_4 \int_0^{2\pi} d\phi_4 \sum_{\lambda_4} (\hat{e}_4 \cdot \hat{e}_{\underset{\sim}{k}})^2 = 8\pi/3 \, ,$$

$$\int_{-1}^{1} d\mu_4 \int_0^{2\pi} d\phi_4 \sum_{\lambda_4} (\hat{e}_4 \cdot \hat{e}_{\underset{\sim}{k}})(\underset{\sim}{k}_2 \cdot \hat{e}_4)(\underset{\sim}{k}_2 \cdot \hat{e}_{\underset{\sim}{k}})^{-1} = 8\pi/3 \, ,$$

where $\sum_{\lambda_4}$ is the sum over polarizations of the photon with momentum $\underset{\sim}{k}_4$.

FOOTNOTES AND REFERENCES

* Based in part on a thesis (A.B.) submitted to the faculty of the graduate school of the University of Wyoming in partial fulfillment of the requirements for the Ph.D. degree, 1970.

† The final stages of this research were completed at Lawrence Radiation Laboratory (Berkeley), while one of us (C.R.S.) was supported by Associated Western Universities, Inc., through contract with the U. S. Atomic Energy Commission and the other (A.B.) was supported by a research assistantship from the Physics Department of the University of Wyoming.

1. F. Mohling and C. R. Smith, submitted to J. Math. Phys.; hereafter referred to as I. Equation (n) of I will be referred to as Eq. (I-n).
2. F. Mohling and W. T. Grandy, Jr., J. Math. Phys. 6, 348 (1965); hereafter referred to as MG.
3. S. Nakai, Nucl. Phys. 63, 131 (1965).
4. W. T. Grandy, Jr., Nuovo Cimento 40, 265 (1965).
5. C. R. Smith, Ph.D. Thesis, University of Colorado, 1967 (unpublished).
6. I. K. Hwang and W. T. Grandy, Jr., Phys. Rev. 177, 359 (1969).
7. W. T. Grandy, Jr., Phys. Rev. 177, 371 (1969).
8. A. Bhowmik, Ph.D. Thesis, University of Wyoming, 1970 (unpublished).
9. Throughout this paper the notation $\delta(t_2^{(-)} - t_1)$ is simplified to $\delta(t_2 - t_1)$.
10. We comment here on the notation. A bar is always placed over quantities associated with $-\underset{\sim}{k}^{\gamma}$ lines. This is necessary since in general the difference between the kernels in Eqs. (3.1) and (3.3) results in two different line factors $\mathcal{G}_{1,1}$ and $\overline{\mathcal{G}}$; for the same reason $\overline{w}_{\gamma}(-\underset{\sim}{k}) \neq w'_{\gamma}(-\underset{\sim}{k})$ [also, see Eqs. (3.30) and (3.31)].

11. Quantities multiplied by $[\Theta(t_2 - t_1) + \nu'_\gamma(\underset{\sim}{k})]$, but which are otherwise independent of t_2 and t_1, are said to be <u>temperature independent</u> (and analogously for $-\underset{\sim}{k}^\gamma$ lines). Thus, in Eq. (3.2) for $Q(t_2,t_1,\underset{\sim}{k}^\gamma)$ [or in Eq. (3.4) for $\overline{\mathcal{M}}_{1,1}(t_2,t_1,-\underset{\sim}{k}^\gamma)$], the counterterms are selected to cancel the temperature independent parts. It should be clear that the counterterm extracts contributions to the interaction potential which are of a single-particle nature [see Eq. (I-5.3)].

12. The mass-renormalization counterterm $S_\alpha(k)$ is suppressed throughout the main text, but is discussed and identified in the Appendix.

13. The approximation in Eq. (3.9) permits us to neglect the particle self-energies $u_\alpha(\underset{\sim}{k})$ so that $w'_\alpha(\underset{\sim}{k}) \simeq w_\alpha(\underset{\sim}{k})$.

14. In arriving at Eqs. (3.28) and (3.29), we must rearrange energy denominators by repeated use of the identity $(ab)^{-1} = [a(a + b)]^{-1} + [b(a + b)]^{-1}$, as well as other analogous identities involving momentum sums.

15. The form in Eq. (3.31) follows from Eq. (3.4); thus, $\overline{w}_\gamma(-\underset{\sim}{k})$ contains no contribution analogous to $u'_\gamma(\underset{\sim}{k})$ - this clarifies further why, in general, $w'_\gamma(-\underset{\sim}{k}) \neq \overline{w}_\gamma(-\underset{\sim}{k})$.

16. W. R. Chappell, W. E. Brittin, and S. J. Glass, Nuovo Cimento <u>38</u>, 1186 (1965).

17. Rayleigh-Schroedinger perturbation theory has been applied to a fully-ionized gas in a pure state, and the expression for the average number of photons has a form analogous to Eq. (4.9).

18. There are some disadvantages in partially diagonalizing the Hamiltonian by means of the Bogoliubov (or any other) transformation, since the explicit appearance of some interaction terms is prevented, thereby obscuring the physical consequences of these interactions. For example, Hwang and Grandy (Ref. 6, Sec. V) were unable to achieve mass-renormalization in the transformed theory, and found it necessary to appeal to the untransformed theory.

19. T. W. B. Kibble, J. Math. Phys. 9, 315 (1968).

20. If iterations of the line factor of a charged particle are introduced, then processes involving the emission and reabsorption of photons by the charged particle are introduced. Such iterations, called radiative corrections, give rise to physical effects as well as to unobservable (system independent) electromagnetic self-energies. The one-particle problem is concerned with the cancellation of these spurious, particle self-energies. The Λ_s-transformation of Sec. IV of MG was developed to treat this problem, and we note here that the counterterm technique of I encompasses the Λ_s-transformation.

21. I. RamaRao and C. R. Smith, submitted to Physical Review.

FIGURE CAPTIONS

Fig. 1. The two generalized master (1,1) graphs of order α_0.

Fig. 2. The six generalized master (1,1) graphs of order α_0^2 which contain ultraviolet divergences.

Fig. 3. The remaining six generalized master (1,1) graphs of order α_0^2 - these graphs do not lead to ultraviolet divergences.

Fig. 4. The four generalized master (2,0) and (0,2) graphs of order α_0.

Fig. 5. The diagrammatic form of the series in Eq. (3.21) for $j = 1$, $\ell = 1$.

Fig. 6. The diagrammatic form of the series in Eq. (3.21) for $j = 1$, $\ell = 2$.

Fig. 7. The diagrammatic form of the series in Eq. (3.21) for $j = 2$, $\ell = 1$.

Fig. 8. The diagrams which, in lowest order, are equivalent to the pair-Hamiltonian approximation.

Fig. 9. The diagrams considered in the calculation of the line factor in Eq. (4.5).

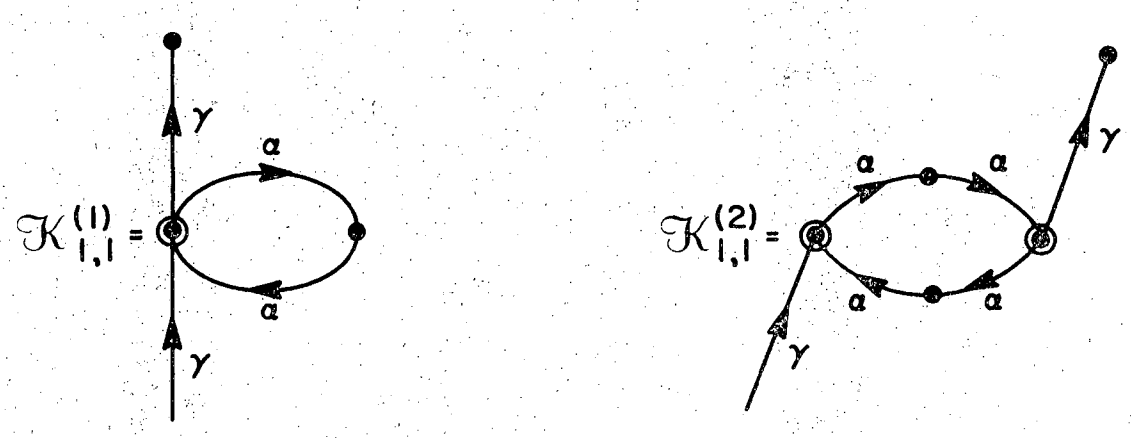

XBL 701-119

Fig. 1

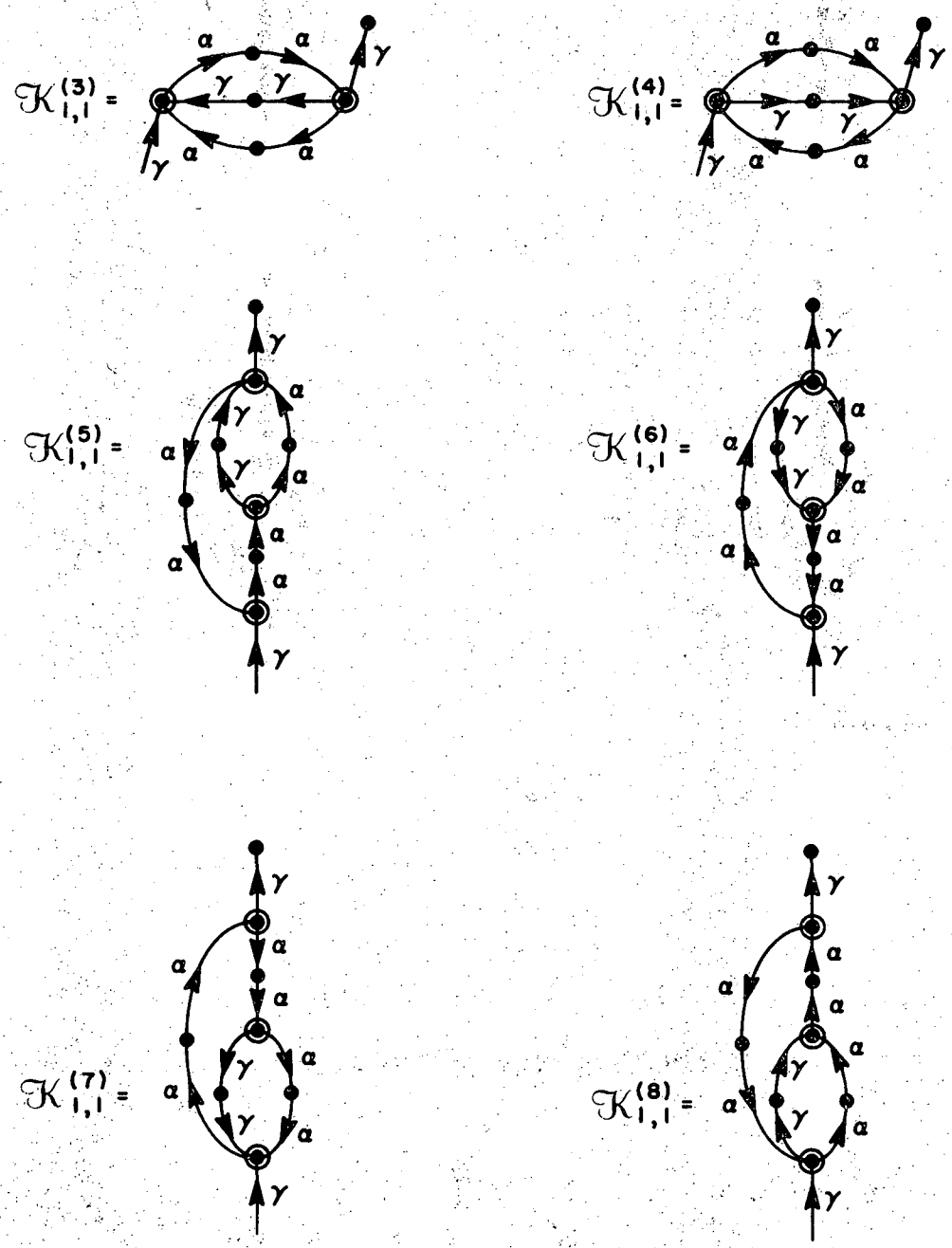

XBL 701-124

Fig. 2

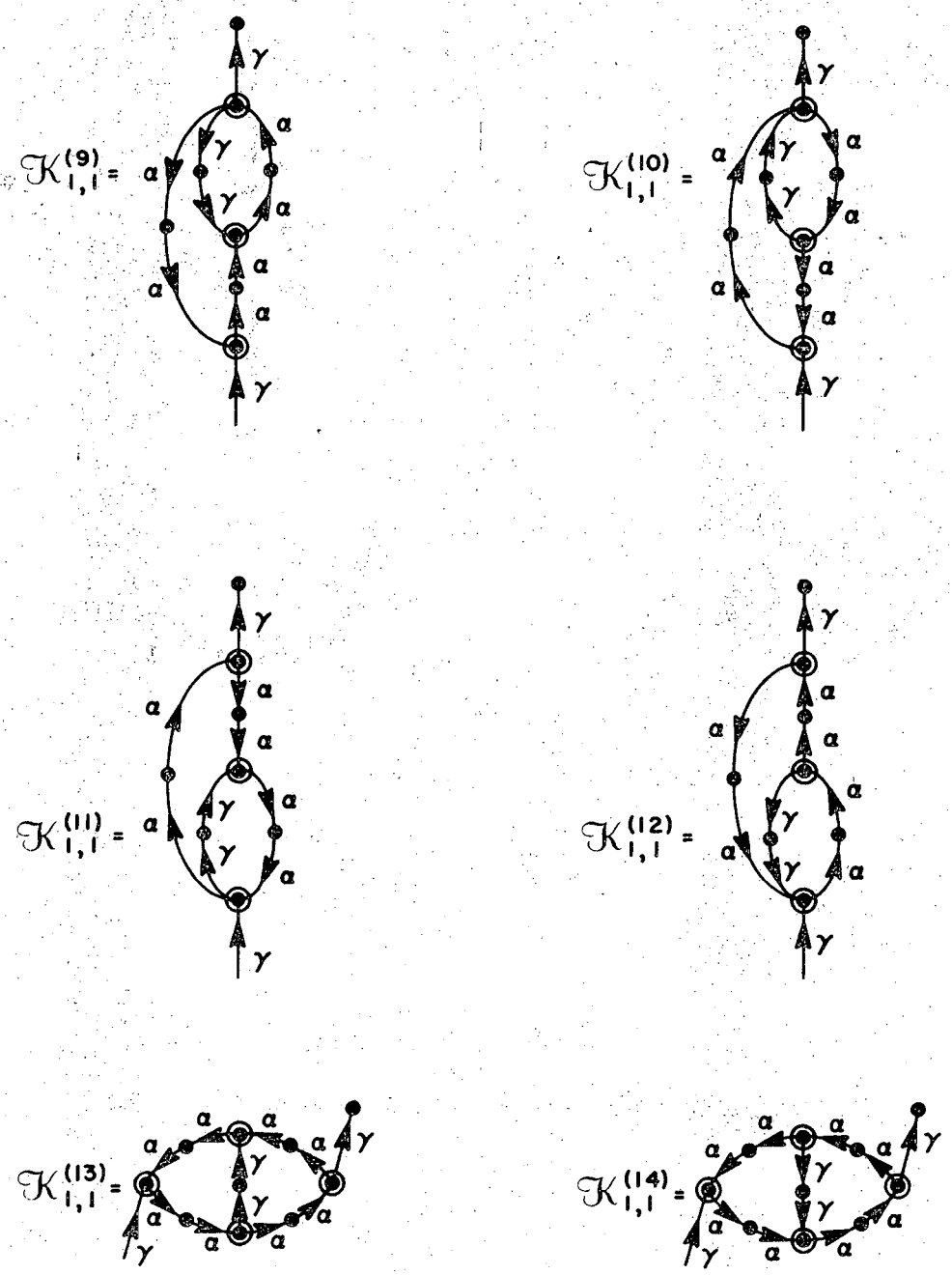

XBL 701-121

Fig. 3

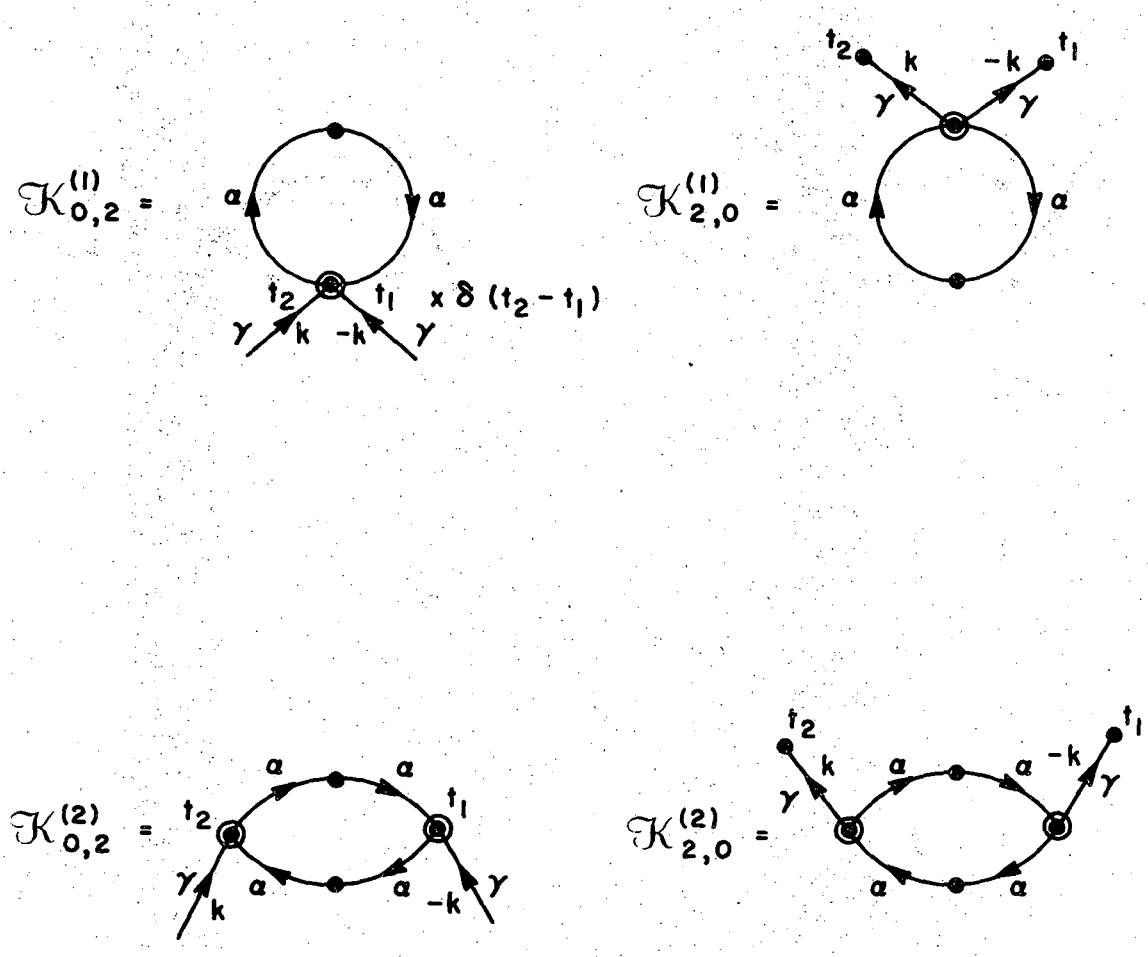

XBL 701-120

Fig. 4

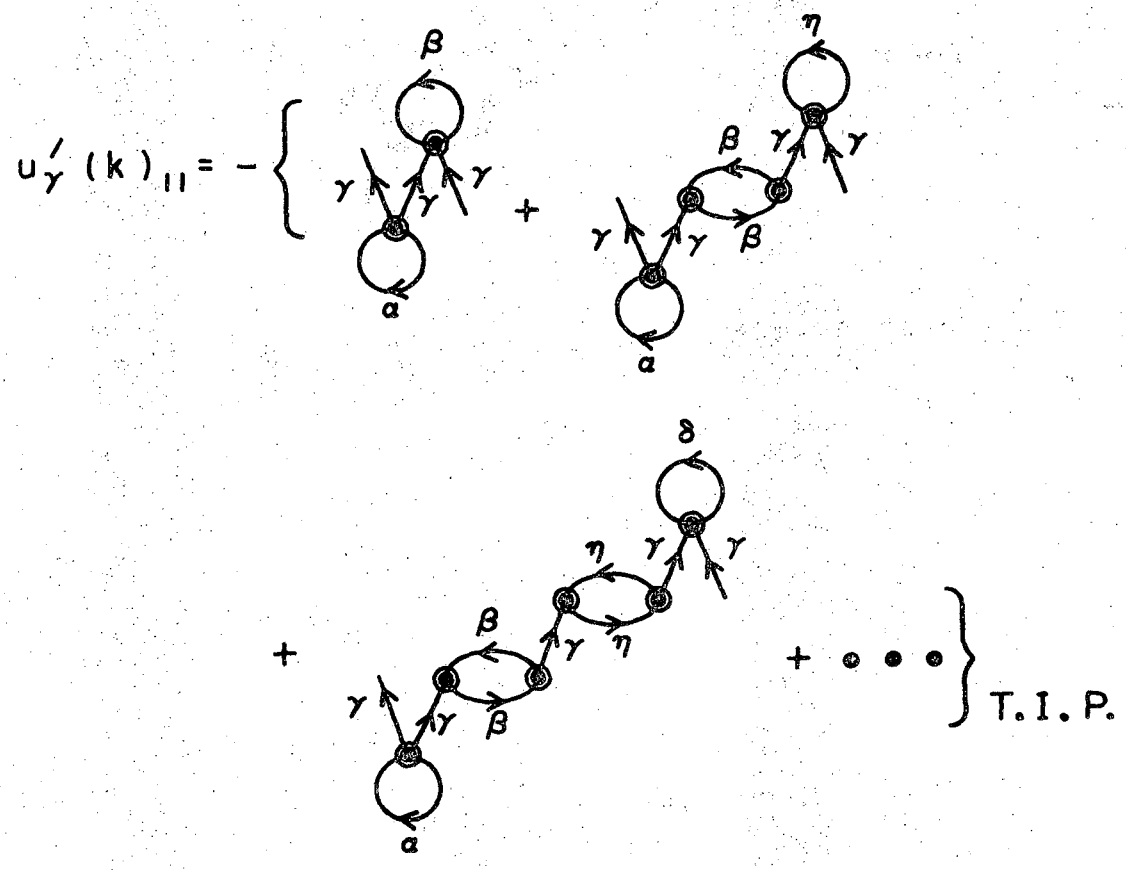

XBL703-2559

Fig. 5

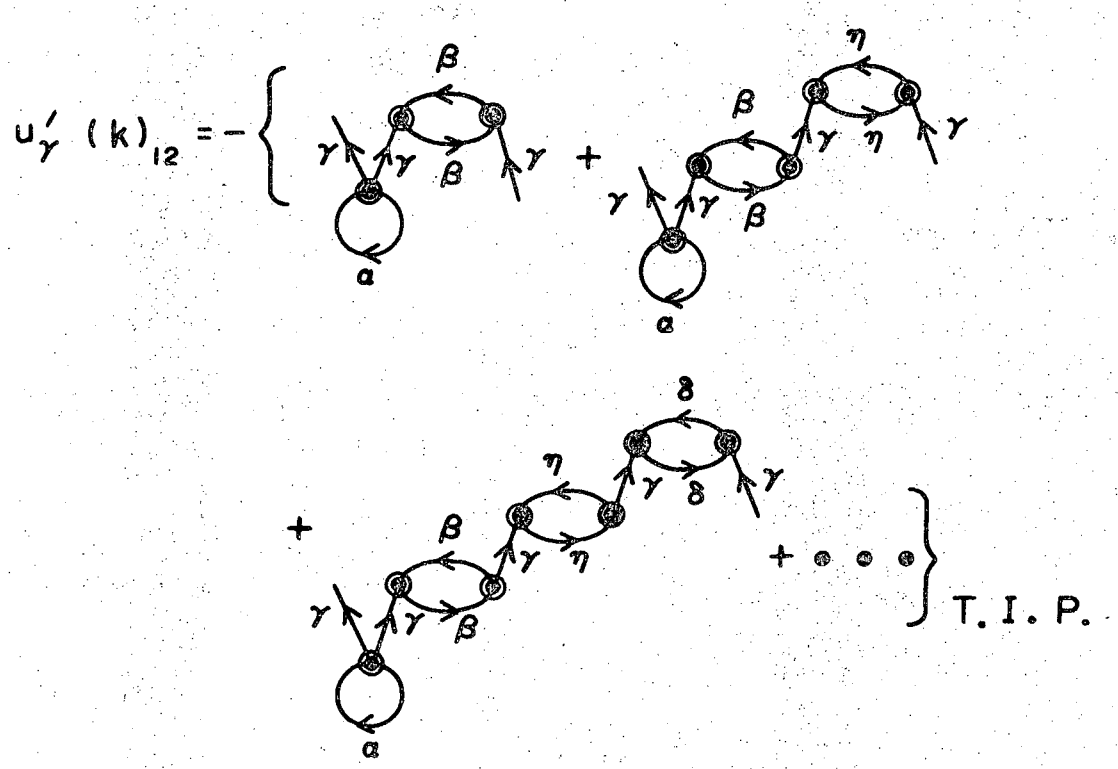

XBL 703-2562

Fig. 6

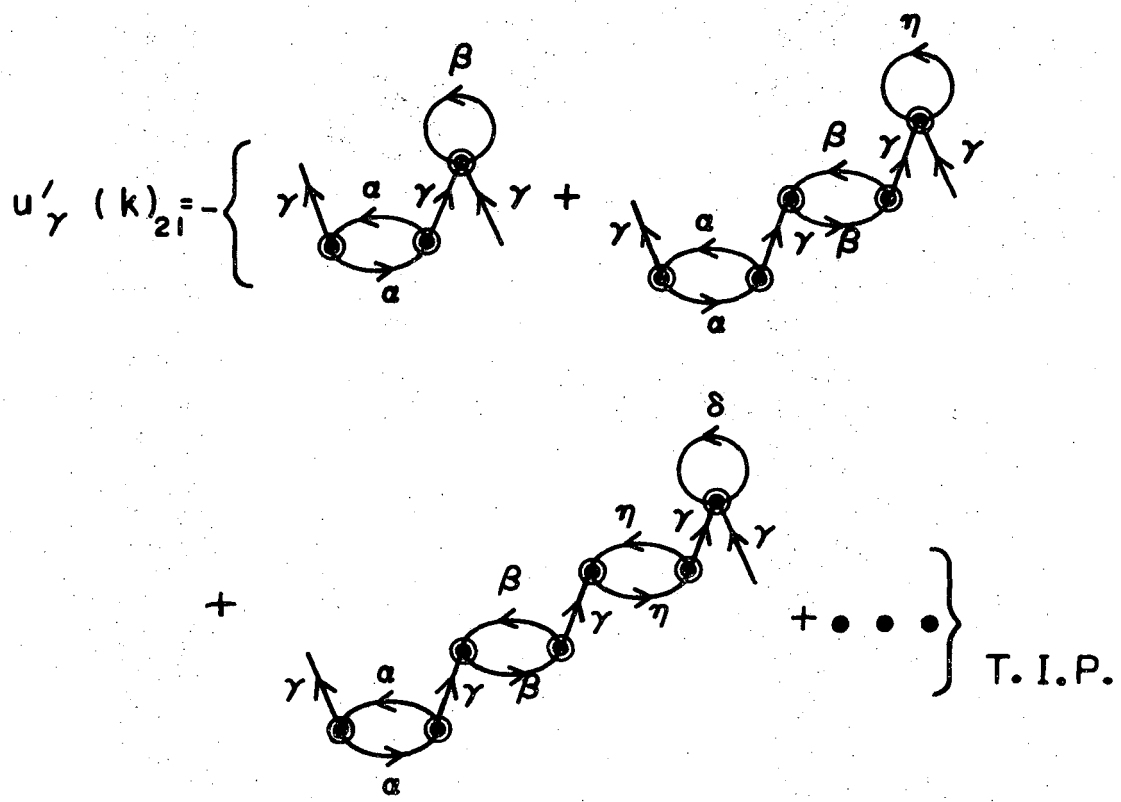

XBL703-2558

Fig. 7

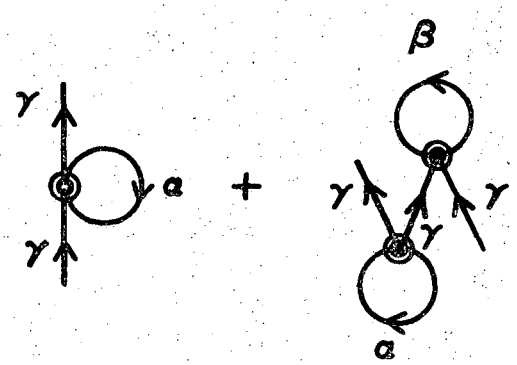

XBL703-2561

Fig. 8

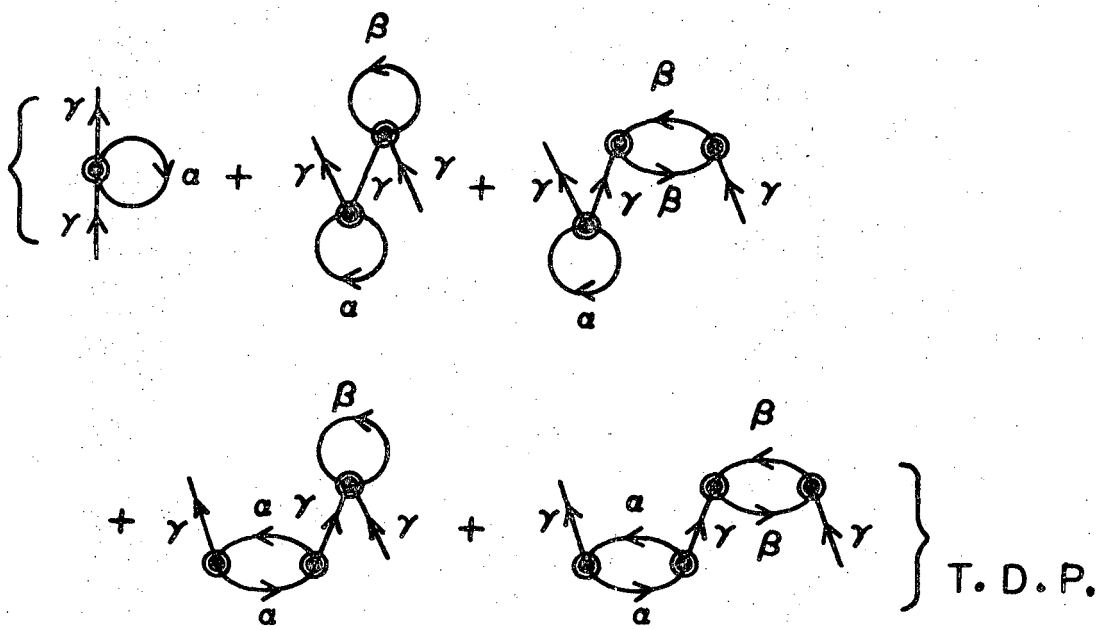

XBL703-2560

Fig. 9

LEGAL NOTICE

This report was prepared as an account of Government sponsored work. Neither the United States, nor the Commission, nor any person acting on behalf of the Commission:

A. Makes any warranty or representation, expressed or implied, with respect to the accuracy, completeness, or usefulness of the information contained in this report, or that the use of any information, apparatus, method, or process disclosed in this report may not infringe privately owned rights; or

B. Assumes any liabilities with respect to the use of, or for damages resulting from the use of any information, apparatus, method, or process disclosed in this report.

As used in the above, "person acting on behalf of the Commission" includes any employee or contractor of the Commission, or employee of such contractor, to the extent that such employee or contractor of the Commission, or employee of such contractor prepares, disseminates, or provides access to, any information pursuant to his employment or contract with the Commission, or his employment with such contractor.

TECHNICAL INFORMATION DIVISION
LAWRENCE RADIATION LABORATORY
UNIVERSITY OF CALIFORNIA
BERKELEY, CALIFORNIA 94720